†Influence of DIBMA polymer length on lipid nanodisc formation and membrane protein extraction

Lauren E. Ball, [‡a] Liam J. Riley, [‡b,c] Waled Hadasha,[a] Rueben Pfukwa,[a] Corinne J. I. Smith[b], Tim R. Dafforn*[c] and Bert Klumperman*[a]

[a.] *Department of Chemistry and Polymer Science, Stellenbosch University, Private Bag X1, Matieland, 7602, Stellenbosch, South Africa.*

[b.] *School of Life Sciences, Gibbet Hill Campus, The University of Warwick, Coventry, CV4 7AL, United Kingdom.*

[c.] *School of Biosciences, University of Birmingham, Edgbaston, Birmingham, B15 2TT, United Kingdom.*

[‡]These co-authors contributed equally to this work.

†Electronic Supplementary Information (ESI) available

Abstract

Polymer-based lipid nanoparticles like SMALPs have revolutionized the study of membrane proteins. More recently, alternative polymers such as poly(diisobutylene-*alt*-maleic acid) (DIBMA) have been used in this field. DIBMA is commonly synthesized via conventional radical copolymerization. In order to study the influence of its chain length on lipid nanodisc formation and membrane protein extraction, we synthesized DIBMA with molar masses varying from 1.2 – 12 kDa via RAFT-mediated polymerization. For molar masses in the range of 3 – 7 kDa, the rate of lipid nanodisc formation was highest and similar to that of SMA and commercially available DIBMA. ZipA solubilization efficiency was significantly higher than for commercially available DIBMA and similar to SMA (circa 75%). Further, RAFT-made DIBMA with a molar mass of 1.2 – 3.9 kDa showed a much cleaner separation on SDS-PAGE, without the smearing that is typically seen for SMA and commercially available DIBMA.

Introduction

Styrene-maleic acid lipid particles (SMALPs) are stable nanoscale complexes of poly(styrene-*co*-maleic acid) (SMA) and lipids that have a disc shape morphology.[1] The complexes assemble in aqueous solution by the intercalation of the phenyl groups of SMA between the acyl chains of lipids perpendicular to the bilayer plane.[2, 3] In the last 10 years these complexes have found significant utility as a support for stabilizing integral membrane proteins.[4-6]

Membrane proteins encapsulated within SMALPs have been shown to be amenable to study by a range of biophysical techniques whilst maintaining a near-native lipid environment. Insertion into SMALPs has enabled membrane proteins to be studied by a number of methods including circular dichroism spectroscopy, nuclear magnetic resonance spectroscopy, analytical ultracentrifugation,[1] small-angle X-ray and neutron scattering, mass spectroscopy,[7] and cryo-electron microscopy.[5]

However, SMA does not represent a universal solution to the study of membrane proteins. The presence of negatively charged maleic acid residues means that the polymer is only soluble at pH > ~6.4, below this the SMALP dissociates and the polymer precipitates. Whilst this still allows for study across the physiological pH range, it does preclude use of SMALPs for various techniques which may require acidic chemistries.[8] SMALP structure is also influenced by divalent cations, which have been shown to bind to the SMALP and cause precipitation of the polymer. Finally, the presence of styrene moieties in the SMA polymer interferes with UV absorbance measurements at 280 nm, a region typically used to determine protein concentrations in solution.[3] These limitations of the SMA copolymer have led to the development of alternative reagents over the past 3 years. The most successful being poly(diisobutylene-*alt*-maleic acid) (DIBMA).[9, 10]

DIBMA is a copolymer made up of aliphatic rather than aromatic hydrophobic groups and has been shown to have similar solubilization properties to that of SMA, being capable of extracting proteins directly from cell membranes.[11] The presence of an aliphatic chain instead of the styrene ring seen in SMA confers a number of benefits, a primary one being lack of interference in spectroscopic studies,

allowing for easier study of membrane proteins solubilized in DIBMA without any contributions towards absorption caused by the polymer belt.

Both the commercial SMA and DIBMA polymers used in membrane protein extraction are produced using conventional radical polymerization which limits the degree of control over molecular weight distribution (MWD) and chain topology.[12] The broad MWD is due to the probability based chain growth process with continuous initiation and termination. In contrast reversible deactivation radical polymerization (RDRP), also known as living radical polymerization, allows for the synthesis of well-defined polymeric architectures with narrow MWDs, predetermined molecular weights and high end-group fidelity as well as allowing for continued chain growth to take place in subsequent polymerization steps. Various types of RDRP are available for the production of well-defined macromolecular architectures, some of which include atom transfer radical polymerization (ATRP), nitroxide-mediated polymerization (NMP) and reversible addition-fragmentation chain transfer polymerization (RAFT). Due to the extensive knowledge that is available regarding the synthesis of SMA via RAFT-mediated polymerization within our research group, RAFT is the RDRP technique of choice for the synthesis of well-defined DIBMA within this paper. RAFT allows for precise control over the chain length distribution as the high rate of the addition/fragmentation reactions in comparison with the rate of propagation leads to one or very few monomer additions per activation cycle, resulting in all polymer chains having a similar degree of polymerisation.[13] While RAFT polymerization allows for the polymerization of an extensive range of functional monomers, it is important to choose an appropriate chain transfer agent (CTA) by careful selection of the Z- and R- group of the CTA, in order to achieve successful control over the polymerization. In general, the use of trithiocarbonates and dithiobenzoates works well for the RAFT polymerization of monomers with vinyl groups conjugated to double bonds, such as MAnh and STY. However, a 1,1-dialkyl substituted monomer has not been copolymerized before with maleic anhydride (MAnh) in a RAFT-mediated reaction. The successful RAFT mediated copolymerization of MAnh with 1-alkenes has previously been reported to yield well-defined polymers through the use of a trithiocarbonate as CTA and thus *S*-butyl-*S′*-(1-phenyl

ethyl) trithiocarbonate (BPT) was chosen as the RAFT agent of choice for the polymerization of diisobutylene (DIB) and MAnh.[14] In this paper we exploit the control provided by RAFT polymerization to explore the influence of DIBMA polymer length on lipid particle formation.

Materials and methods

Materials

Maleic anhydride (MAnh) briquettes (99%, Sigma-Aldrich) and 2,2'-azobis(2-butyronitrile) (AIBN) were purified via recrystallization from toluene and methanol respectively and were dried under vacuum overnight. 2,4,4-Trimethyl-1-pentene (diisobutylene, DIB) (99%, Sigma-Aldrich); 2-butanone (≥99%, Sigma-Aldrich), Na_2CO_3 (98%, Merck), 1,3,5-trioxane (≥99%, Sigma-Aldrich), 1-butanethiol (97%, Fluka), carbon disulphide (99%, Sigma-Aldrich), triethylamine (99%, Sigma-Aldrich), 1-bromoethylbenzene (97%. Sigma-Aldrich), $CDCl_3$ (99.9%, MagniSolv) and acetone-d_6 (99.9%, MagniSolv) were used as received. Chloroform was distilled prior to use. The RAFT agent *S*-butyl-*S'*-(1-phenyl ethyl) trithiocarbonate (BPT) was synthesized as described in literature.[15]

Nomenclature

In all experiments, DIBMA polymers were given a name denoting the method used to synthesize the parent DIBMAnh copolymer (i.e. 'R' for RAFT synthesized and 'C-' for conventional free radical polymerization synthesized DIBMAnh copolymers) followed by the approximate experimental overall number average degree of polymerization). For example, entry 1, Table 1, i.e. C-D91 represents a DIBMAnh parent copolymer prepared by free radical copolymerization with a degree of polymerization, i.e. D, of 91, whilst entry 1 Table 2, i.e. R-D12 represents a RAFT-made DIBMAnh parent copolymer with D ≈ 12.

BPT synthesis

1-Butanethiol (5.01 g, 56 mmol), carbon disulphide (8.45 g, 111 mmol) and chloroform (40 mL) were added to a 250 mL round bottom flask fitted with a Teflon coated stirrer bar. Triethylamine (11.22 g, 111 mmol) was added dropwise while stirring and the reaction was allowed to proceed at room temperature for 5 hours. 1-Bromoethylbenzene (10.36 g, 56 mmol) was then added dropwise while stirring and the reaction mixture was subsequently allowed to stir overnight at ambient conditions. BPT was isolated from the reaction mixture by successively washing with distilled deionized (DDI) water (2 × 50 mL), H_2SO_4 (2 M, 2 × 50 mL), DDI water (2 × 50 mL) and saturated brine (2 × 50 mL). The mixture was then dried overnight by stirring over anhydrous $MgSO_4$ and subsequently filtered and concentrated to yield a viscous yellow-orange oil, (14.84 g, 98 %), which was determined to be 96% pure via ^{1}H NMR spectroscopy.

^{1}H NMR (300 MHz, $CDCl_3$) δ = 7.24-7.41 (m, 5H, aromatic), 5.36 (q, *J* = 5.3 Hz, 1H, -SC**H**-), 3.35 (t, *J* = 5.7 Hz, 2H, -SC**H**$_2$-), 1.77 (d, *J* = 5.3 Hz, 3H, -S-CH-C**H**$_3$), 1.68 (q, *J* = 5.6 Hz, 2H, -CH$_2$-C**H**$_2$-CH$_2$-), 1.43 (sext, *J* = 5.6 Hz, 2H, -CH$_2$-C**H**$_2$-CH$_3$), 0.94 (t, *J* = 5.5 Hz, 3H, -CH$_2$-C**H**$_3$)

^{13}C NMR (75 MHz, $CDCl_3$) δ = 14.18 (**C**H$_3$CH$_2$CH$_2$CH$_2$-), 21.93 (**C**H$_3$CH), 22.65 (CH$_3$**C**H$_2$CH$_2$CH$_2$-), 30.58 (CH$_3$CH$_2$**C**H$_2$CH$_2$-), 37.08 (-**C**H$_2$-S), 50.63 (**C**H), 128.22 (*p*-Ph, **C**H), 128.26 (*m*-Ph, **C**H), 129.19 (*o*-Ph, **C**H), 141.73 (Ph, **C**), 223.66 (**C**S$_3$)

General procedure for the synthesis of DIBMAnh

Table 1. Conventional radical copolymerization experiments for the production of DIBMAnh

Sample	T (°C)	Initiator (mol %)	Total conversion (%)	[b] DIB conversion (%)	[b] MAnh conversion (%)	[c] M_n (kDa)	*Đ*
C-D91	70	0.5	24 [a]	-	-	9 .6	2.98
C-D100	80	0.5	46 [a]	-	-	10.5	2.02
C-D184	80	0.05	75	85	64	19.4	2.10

C-D97	80	1.5	82	92	73	10.2	2.49
C-D62	80	5	97	97	94	6.6	1.96

a- Conversion determined gravimetrically via precipitation of DIBMAnh in isopropanol

b- Conversion determined using ^{1}H NMR spectroscopy and an internal reference (1,3,5-trioxane)

c- Molecular weights determined using SEC with DMF as the mobile phase and PMMA calibration standards

In a typical conventional radical polymerization experiment (Table 1, C-D62), MAnh (3.06 g, 31.2 mmol), DIB (3.50 g, 31.2 mmol), AIBN (0.51 g, 3.1 mmol), 1,3,5-trioxane (0.38 g, 4.2 mmol) and 2-butanone (15 mL) were added to a 50 mL 2-necked pear-shaped flask fitted with a magnetic stirrer bar, condenser and bubbler. A sample (0.1 mL) was withdrawn at time t=0. The mixture was degassed by purging with argon gas for 45 minutes and then submerged in an oil bath at 80 °C for 24 h. At time t=24 h, a sample (0.1 mL) was withdrawn, and the polymerization terminated by cooling the flask in an ice-water bath and introducing oxygen into the reaction mixture. For samples C-D91, C-D100, C-D184 and C-D97 the same general procedure was followed but either the temperature was changed (70 °C) or the amount of initiator was changed.

Table 2. RAFT mediated copolymerization experiments for the production of DIBMAnh

Sample	**M_n target (kDa)**	**Total conversion (%)**	**[b] $M_{n,th}$ (kDa)**	**[c] DIB conversion (%)**	**[c] MAnh conversion (%)**	**[d] M_n SEC (kDa)**	**M_n NMR (kDa)**	***Đ***
R-D12	2.4	39 [a]	1.1	-	-	1.2	1.3	1.45
R-D20	2.4	63	1.6	71	55	3.2	2.1	1.24
R-D22	2.4	73	1.8	73	72	2.6	2.4	1.28

R-D32	5.4	67	3.8	66	68	2.4	3.4	1.50
R-D37	5.4	64	3.6	64	63	5.5	3.9	1.28
R-D41	5.5	66	3.8	72	61	4.7	4.4	1.33
R-D66	15.0	65	9.9	74	55	9.8	7.0	1.31
R-D88	20.5	22 [a]	4.9	-	-	9.1	9.3	1.70
R-D96	20.6	33 [a]	7.2	-	-	13.8	10.1	1.27

a- Conversion determined gravimetrically via precipitation of DIBMA in isopropanol

b- Theoretical M_n calculated using individual DIB and MAnh conversions

c- Conversion determined using ^{1}H NMR spectroscopy and an internal reference (1,3,5-trioxane)

d- Molecular weights determined using SEC with DMF as the mobile phase and PMMA calibration standards

For a typical RAFT polymerization (Table 2, R-D20), MAnh (2.9 g, 30.0 mmol), DIB (3.4 g, 30.1 mmol), AIBN (0.1 g, 0.6 mmol), BPT (0.81 g, 3.0 mmol), 1,3,5-trioxane (0.31 g, 3.5 mmol) and 2-butanone (15 mL) were added to a 3-neck round bottom flask fitted with a magnetic stirrer bar, condenser and bubbler. A sample (0.1 mL) was withdrawn at t=0 h. The mixture was then degassed by purging with argon gas for 45 minutes before being immersed in an oil bath at 80 °C for 24 h. At time t=24 h, a sample (0.1 mL) was withdrawn before the round bottom flask was cooled down in an ice-water bath and the flask opened to expose the mixture to oxygen. DIBMA was isolated from the reaction mixture by precipitating the copolymer in isopropanol (80 mL) and centrifuging the mixture at 4500 rpm for 5 minutes in order to obtain the polymer pellet. This pellet was then washed with isopropanol and centrifuged again. The resulting pellet was dried under vacuum at 40 °C and the dry DIBMAnh analyzed using size exclusion chromatography (SEC), ^{1}H NMR spectroscopy and ATR-FTIR spectroscopy. For samples R-D12, R-D22, R-D32, R-D37, R-D41, R-D66, R-D88, R-D96, R-D37 and R-D54 the same general procedure was followed but either the ratio of BPT to monomer was altered for the production of a

variety of molecular weights (calculated using Equation S1, Supporting Information) or the ratio of MAnh and DIB was varied to investigate the alternating nature of the copolymerization. For all RAFT polymerizations the ratio between RAFT agent and initiator was kept constant 5:1. A typical kinetic experiment would involve the withdrawal of samples (0.1 mL) under argon at set time intervals (30 min, 1 h, 2 h, 4 h, 6 h, 8 h, and 24 h) which were then exposed to air and quenched in liquid nitrogen to terminate polymerization. These samples were then added to deuterated acetone (0.75 mL) and individual monomer conversions determined using ^{1}H NMR spectra with 1,3,5-trioxane as the internal standard (Equation S2).

General procedure for the hydrolysis of DIBMAnh

A stock solution of Na_2CO_3 (1 M, 250 mL) was prepared and used for the hydrolysis of samples C-D62, R-D12, R-D20, R-D32, R-D37, R-D66, R-D88 and R-D96. The DIBMAnh was weighed off into 50 mL round bottom flasks and a calculated volume of Na_2CO_3 solution added, such that 2 equivalents of Na_2CO_3 to MAnh units were used. These flasks were fitted with magnetic stirrer bars and the mixture stirred at 80 °C for 24 h. The reaction mixture is initially heterogeneous as DIBMAnh is insoluble in water, thus the complete solubilization of DIBMAnh is an indication of DIBMA production. After 24 h the contents of the flask were transferred to dialysis tubing (3500 MWCO) and allowed to stir in water for 1.5 h to remove residual Na_2CO_3. The tube was removed from water and stirred in methanol for 1.5 h resulting in the partial precipitation of DIBMA. This mixture was transferred to a 250 mL round bottom flask and the methanol removed under reduced pressure. The isolated DIBMA was then dried in a vacuum oven at 40 °C for 24h. The successful production of DIBMA was confirmed via ATR-FTIR spectroscopy and the retention of the RAFT moiety at the chain ends was assessed using UV/Vis spectroscopy.

Characterization of DIBMAnh and DIBMA

^{1}H NMR spectra were obtained using a Varian VXR-Unity (400 MHz) spectrometer. The DIBMAnh copolymers were dissolved in either $CDCl_3$ or acetone-d_6, where the deuterated solvent used is specified with the reported data. Attenuated total reflectance infrared spectroscopy (ATR-FTIR) was

performed using a Thermo Scientific Nicolet iS10 Smart iTR, using 200 scans over the wavelength range of 600 – 4000 cm^{-1}. SEC was performed using DMF SEC where all samples made for this analysis are prepared in *N*,*N*-dimethylformamide (DMF) (Sigma-Aldrich, Chromosolv® Plus, for HPLC ≥99.9%) with 0.05 M LiBr. The samples were analyzed using a set-up consisting of a Waters 717 plus auto-sampler with a Waters in-line degasser AF connected to a Shimadzu LC-10AT pump. The column set-up consisted of a pre-column (1×PSS GRAM column) with a 10 µm particle size and dimensions of 8.0×50 mm; analytical columns 1×PSS GRAM (10 µm particle size, 100 Å pore size, 8.0×300 mm) and 2×PSS GRAM columns (10 µm particle size, 3000 Å pore size, 8.0×300 mm). A Waters 410 differential refractometer and a Waters 2487 dual wavelength absorbance detector were connected in series. The flow rate was 0.8 mL/min and the columns were kept at 40 °C. The SEC system was calibrated using low dispersity poly(methyl methacrylate) calibration standards. UV/Vis spectra were obtained using a Specord 210 Plus UV/Vis spectrophotometer in the wavelength range 190-1100 nm using water as the solvent with DIBMA concentrations of 5 mg/mL.

Solubilization of DMPC liposomes by DIBMA

A stock solution of 1,2-dimyristoyl-sn-glycero-3-phosphocholine (Avanti Polar Lipids; 14:0 PC (DMPC)) liposomes were prepared by suspension of dry lipid powder in a methanol solution, before evaporation and dissolution to a concentration of 100 mg/mL in 20 mM Tris-HCl, 200 mM NaCl, pH 8.0, this stock solution was stored at -20 °C until use. Liposomes were produced by sonication in a bath sonicator for 1 min, followed by 4 freeze-thaw cycles and extrusion through a 100 nm filter to generate a sample of homogenous liposomes. Working solutions of DMPC liposomes were produced by dilution of the 100 mg/mL stock solution in 20 mM Tris-HCl, 200 mM NaCl, pH 8.0.

Solutions of SMA and DIBMA were prepared by dissolving the polymers to a concentration of 50 mg/mL in 20 mM Tris-HCl, 200 mM NaCl, pH 8.0. A 0.5 mg/mL solution of DMPC liposomes was prepared by dilution of the 100 mg/mL DMPC stock solution in 20 mM Tris-HCl, 200 mM NaCl, pH 8.0, followed by sonication in a bath sonicator for 15 min. Polymer induced liposome dissolution was monitored by measuring the optical density of 620 nm light of a solution of liposomes using a Cary

100 UV-Vis spectrophotometer. A cuvette containing 500 µL of the 0.5 mg/mL liposome solution was placed in the spectrophotometer and allowed to equilibrate for 1 min before the addition of SMA or DIBMA solutions to a final concentration of 0.15 mg/mL. The optical density of the sample was then followed over a period of 10 min. All measurements were performed at 25 °C.

Characterization of DIBMA nanodiscs

Nanodiscs were produced by addition of SMA or DIBMA in 20 mM Tris-HCl, 200 mM NaCl, pH 8.0 at 5% (w/v) in a 3:1 (w/w) polymer/lipid ratio to DMPC liposomes in 20 mM Tris-HCl, 200 mM NaCl, pH 8.0 followed by equilibration overnight at 25 °C. Nanodiscs were purified where necessary by means of SEC using an ÄKTA pure protein purification system with a Superdex 200 Increase 10/300 GL (GE Healthcare) equilibrated in 20 mM Tris-HCl, 200 mM NaCl, pH 8.0 at 4 °C. A flow rate of 0.5 mL/min was used and elution profiles determined by measuring the absorbance at 280 nm and 260 nm.

Negatively stained SMA and DIBMA DMPC nanodiscs were visualized with transmission electron microscopy (TEM). 5 µL aliquots of nanodiscs produced at 3:1 polymer:lipid were adsorbed to glow-discharged 300 mesh Formvar carbon copper grids (Agar Scientific) and excess sample removed after 120 s with filter paper (Whatman). Prior to staining, grids were washed with water for 10 s; excess water was removed with filter paper. Grids were stained with 5 µL of 2% (w/v) uranyl acetate for 60 s and excess staining solution removed with filter paper. Grids were air-dried at room temperature and imaged with a Jeol2100Plus TEM operating at an acceleration voltage of 200 kV. Shape factors (diameter and area) of ellipses fitted to particles were analyzed and determined using ImageJ.

Dynamic light scattering (DLS) measurements were conducted using a Malvern Nano S operating with a detector angled at 173 ° from the incident ray direction. 100 µL aliquots of purified nanodiscs were placed into disposable cuvettes and capped to prevent dust contamination. For each sample 10 measurements were performed with each being averaged over 10 runs of 10 s. All measurements were performed at 25 °C.

Stability of DIBMA nanodiscs

Solubilization of *E. coli* ZipA membranes by DIBMA

E. coli membranes were produced as detailed in the paper by Lee *et al.* (2019)[16] using BL21 Star™ (DE3) Chemically Competent *E. coli* transformed and induced for high-level expression of His_6 tagged (C-terminus) ZipA in 50 mM Tris-HCl, 500 mM NaCl, 10% glycerol (v/v), pH 8.0.

Solutions of SMA and DIBMA at 5% (w/v) in resuspension buffer were added to an equal volume of the resuspended pellet and left to incubate at room temperature for 2 hours. After incubation 1 mL aliquots of the samples were centrifuged at 100,000×g for 45 min to separate soluble and insoluble fractions, insoluble fractions were resuspended in 1 mL resuspension buffer and analyzed by SDS-PAGE and subsequent densitometric analysis performed in ImageJ.

Results and discussion

DIBMAnh synthesis- Conventional radical polymerization

Conventional radical polymerizations were conducted to optimize the reaction conditions for RAFT polymerization in order to maximize monomer conversion. Initially, the reaction temperature was optimized by performing two copolymerizations, one at 70 °C and the other at 80 °C. As expected, the copolymerizations conducted at 80 °C yielded a higher conversion (**Table 1**) and thus all RAFT polymerizations were performed at this reaction temperature. Variation of the [monomer]:[initiator] ratio for conventional radical polymerizations allowed for the production of DIBMAnh copolymers with different M_n values. The copolymerization that utilized a lower initiator concentration yielded higher M_n values while higher initiator concentrations allowed for the production of lower molecular weight copolymers. ^{1}H NMR spectroscopy was utilized for monomer conversion determination, with the use of an internal reference (1,3,5-trioxane). Upon determination of comonomer conversion for samples C-D184 and C-D97, it was noted that a ~20% difference in conversion could be observed between MAnh and DIB. This turned out to be due to unintended evaporation of DIB during degassing or during the polymerization. Optimization of the experimental procedure, by ensuring the water

running through the condenser was 0 °C, allowed for decreased DIB evaporation which led to the expected equal conversion of MAnh and DIB (Figure S1, Supporting Information).

DIBMAnh synthesis- RAFT polymerization

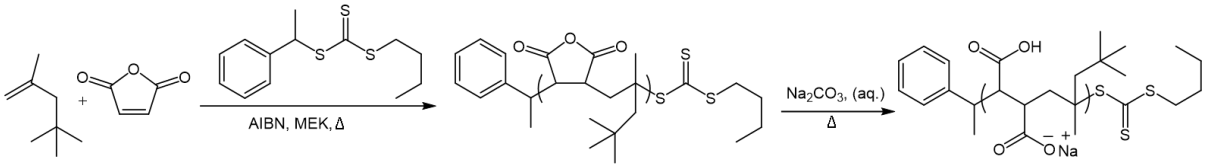

Scheme 1. BPT RAFT-mediated copolymerization of MAnh and DIB and subsequent DIBMAnh hydrolysis using aqueous Na_2CO_3 to produce DIBMA.

For RAFT copolymerizations (Scheme 1), different molecular weights were synthesized (R-D12, R-D20, R-D22, R-D32, R-D37, R-D41, R-D66, R-D88 and R-D96, Table 2) and copolymerizations conducted using optimized reaction conditions. For samples R-D12, R-D88 and R-D96 conversion was determined gravimetrically and due to the loss of polymer during this process, reported conversions are significant underestimations of the true values. For all other RAFT experiments, conversion was determined using ^{1}H NMR spectroscopy and relatively high monomer conversions were obtained.

The molecular weight dispersity (*Đ*) of DIBMAnh obtained via RAFT copolymerization was determined to be relatively low suggesting that a narrow distribution of polymer chain lengths was produced. For sample R-D41 (**Table 2**) a molecular weight of 5 500 g/mol was targeted and the polymerization was conducted over 24 h. Samples were taken at specified time intervals and analyzed using SEC and ^{1}H NMR in order to track comonomer conversion, molecular weight and *Đ*. M_n increased linearly with conversion supporting the livingness of the polymerization system (Figure 1). Based on these results, it was noted that no further increase in molecular weight was achieved after eight hours due to the depletion of AIBN.

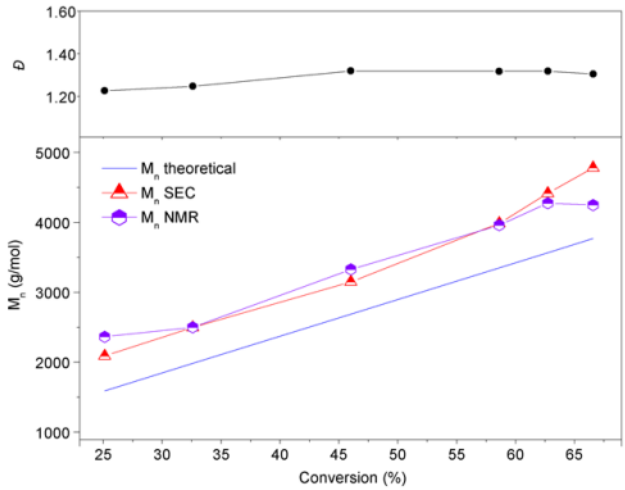

Figure 1. M_n and dispersity vs monomer conversion for the RAFT mediated polymerization of DIB and MAnh to produce R-D41

A gradual decrease in SEC elution volume can be observed, with a slight up-turn at high elution volumes as a result of the overlap of the DIBMAnh SEC curve with that of the flow marker (Figure S2). In addition to the gradual increase in molecular weight, the isolated DIBMAnh was shown to have a narrow molecular weight distribution, thus suggesting that control over the polymerization had been achieved. A difference in comonomer conversion can be observed, due to minimal evaporation of the DIB comonomer, but analysis of the isolated DIBMAnh via ^{1}H NMR spectroscopy revealed approximately equal number of comonomer units (Figure 2). A slight discrepancy can be observed when comparing the values obtained for the molecular weight from the ^{1}H NMR and SEC analyses and this can be attributed to the fact that PMMA calibration standards were used which potentially have a different hydrodynamic volume in solution compared to DIBMAnh. As the molecular weights determined via ^{1}H NMR spectroscopy corresponded well to the theoretical M_n values, these molecular weights were utilized as an indication of polymer chain length in subsequent experiments. Most polymerizations yielded relatively equal comonomer conversions and analysis of the isolated DIBMAnh copolymers using ^{1}H NMR spectroscopy showed approximately equal incorporation of the DIB and MAnh monomers.

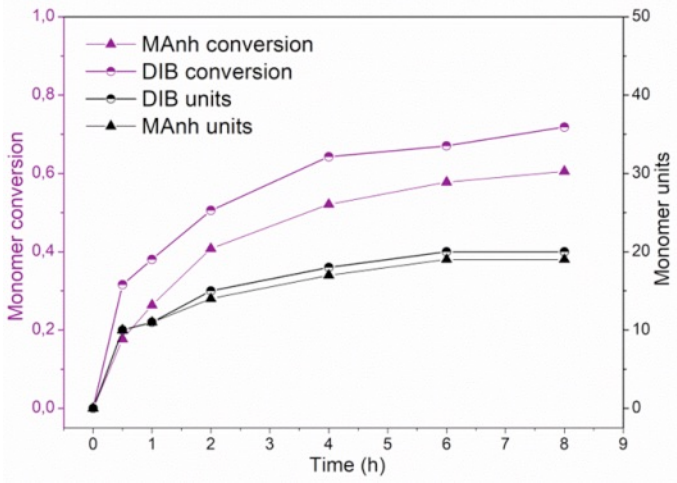

Figure 2. Monomer conversion & monomer units vs time for the RAFT mediated polymerization of DIB and MAnh to produce R-D41.

This suggests the copolymer is alternating in nature as the comonomers are not expected to homopropagate due to their limited intrinsic reactivity. 1-Alkenes, such as DIB, supposedly are only able to polymerize via RDRP or FRP in the presence of a comonomer with a double bond of significantly different polarity, in this case MAnh, resulting in a polarity activation phenomenon thus allowing for the production of alternating copolymers.[14] To confirm the alternating character of the DIBMAnh copolymers, different comonomer ratios were investigated (Table S1). For both R-D37A and R-D54A, monomer conversion was limited by the altered comonomer ratio and analysis of the isolated DIBMAnh copolymers showed that approximately equal numbers of comonomer units had been incorporated. These results would suggest that all DIBMAnh copolymers are alternating in nature, even when variable comonomer ratios are used. Overall, DIBMAnh copolymers of a variety of molecular weights could be synthesized, producing copolymers of well-defined molecular weight and molecular weight dispersity, both of which play an intrinsic role in the optimization of the membrane solubilization process.

DIBMAnh hydrolysis

DIBMAnh copolymers C-D62, R-D12, R-D20, R-D32, R-D37, R-D66, R-D88 and R-D96 were converted to DIBMA via the hydrolysis of the MAnh units using Na_2CO_3 (see Scheme 1). The isolated DIBMA copolymers were analyzed using ATR-FTIR spectroscopy. Successful hydrolysis was characterized by the disappearance of the anhydride stretches at 1849 cm^{-1} and 1772 cm^{-1}, the appearance of the broad carboxylic acid peak at 3679-3035 cm^{-1} and the appearance of a carbonyl peak with shoulder at 1550 cm^{-1} and 1660 cm^{-1} respectively which arises from the combination of asymmetric and symmetric stretches of carboxylate salts, traditionally found at approximately 1600 cm^{-1} and 1400 cm^{-1} respectively (Figure 3A).

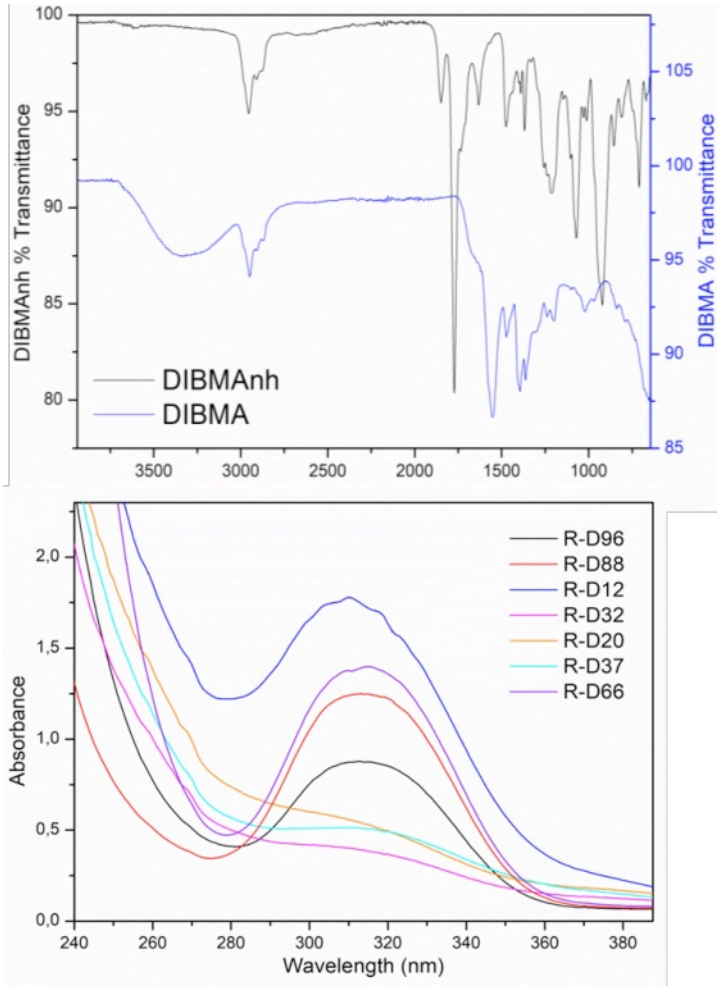

Figure 3. ATR-FTIR comparison between DIBMAnh and DIBMA (top), UV/Vis analysis of DIBMA (bottom).

DIBMA was also analyzed using ^{1}H NMR spectroscopy and the successful hydrolysis of the MAnh units was confirmed via the complete shift of the proton signal from 4.02-3.25 ppm, due to MAnh's methine protons, to 3.17-2.45 ppm, due to maleic acid's methine protons (Figure S3). The hydrolysis of DIBMAnh was carried out in basic aqueous conditions with heating, thus the partial removal of RAFT moieties at the ω-chain ends is not unexpected due to the known hydrolytic instability of RAFT Z end-groups in aqueous alkaline conditions, exacerbated by elevated temperatures.[17] It is likely that the extent to which RAFT moieties are cleaved from DIBMA chains can be influenced by a variety of factors, including the identity of the terminal monomer (i.e. MAnh or DIB), adjacent to the RAFT Z end-group. As the quantitative analysis of end group retention is not within the scope of this work, a qualitative analysis was conducted via UV/Vis spectroscopy. All DIBMA samples analyzed exhibited absorption peaks at ~310 nm (Figure 3B), due to the π – π* transition of the trithiocarbonate moiety of the RAFT Z end-groups,[18] indicating the (partial) retention of the RAFT Z end-groups. The absence of a direct correlation between DIBMA molar mass and UV peak intensity seems to suggest that the degree of end group retention varies among the different samples.

Analysis of the performance of DIBMA variants

To assess the performance of DIBMA variants in the formation of polymer-lipid particles tests were performed on each sample. These included assessing the rate of solubilization of pure lipid (to produce a nanoparticle). If variants produced lipid nanoparticles these particles were then analyzed using dynamic light scattering and electron microscopy to determine if the particle size and shape differed from that formed using the commercial form of DIBMA. The influence of both pH and divalent cation concentration on nanoparticle formation were also assessed. Finally, the efficiency of each polymer in extracting a protein (with local lipid environment) was measured.

Liposome dissolution by DIBMA

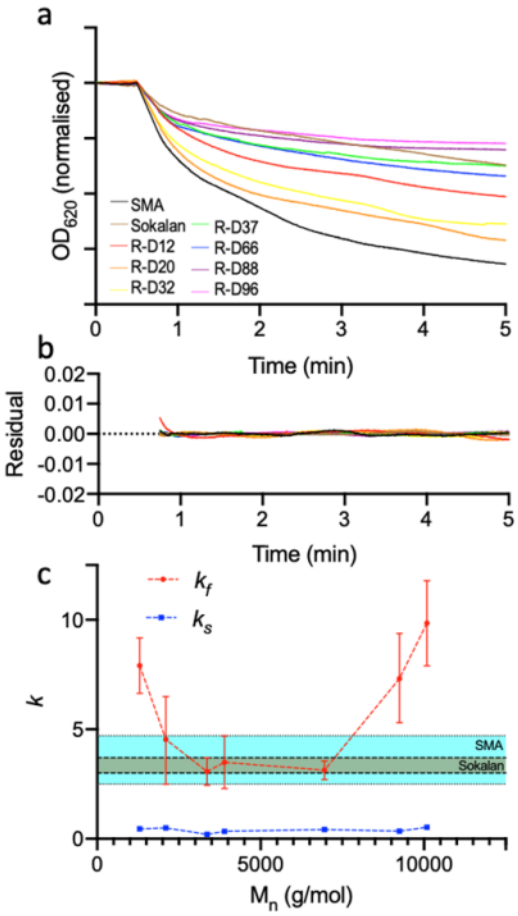

Figure 4. Turbidimetric analysis of solubilization of DMPC liposomes by amphipathic copolymers. (a) Optical density traces for DMPC liposomes upon addition of SMA, Sokalan-derived DIBMA and RAFT DIBMAs of increasing M_n. Liposomes were allowed to equilibrate before addition of copolymer at t = 40 s. A two-phase decay model was used to fit the data (Equation 3) with (b) showing the resulting residuals and (c) representing the rate constants derived from the fitted data plotted as a function of the M_n of the RAFT DIBMA used in solubilization. Points represent the mean of three experiments with error bars representing SEM. The SEM of the k_f of SMA and Sokalan are represented as the cyan and brown highlighted regions, respectively.

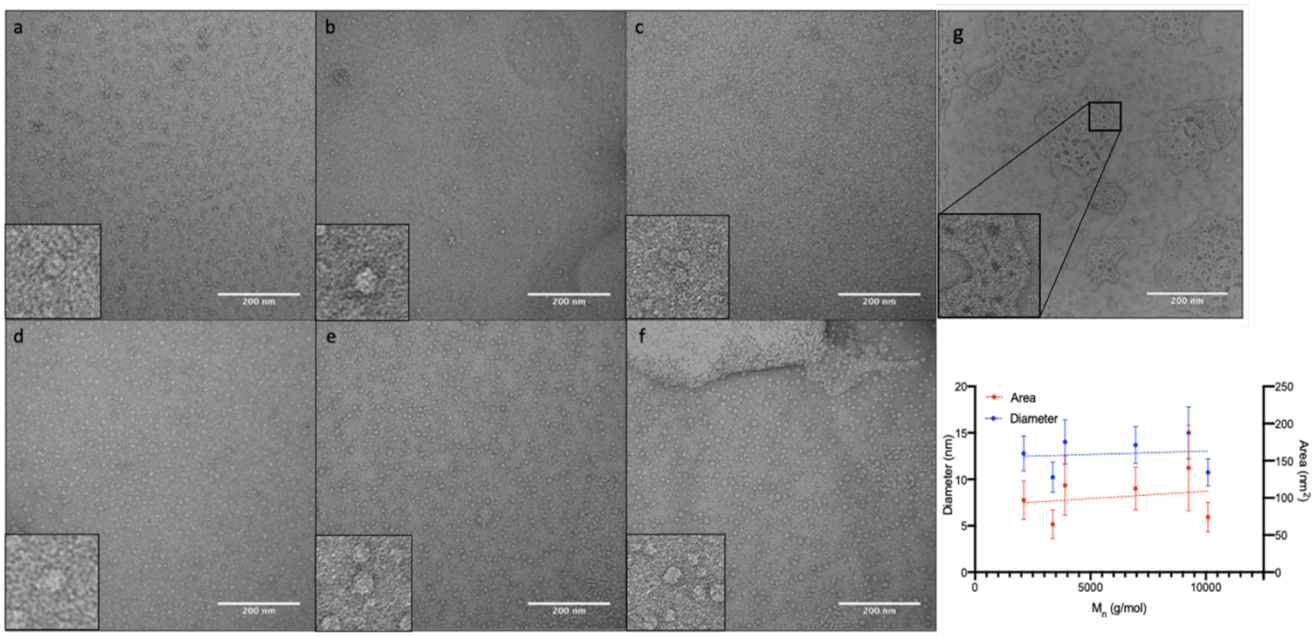

Figure 5- Representative transmission electron micrograph (TEM) of DMPC liposomes solubilized using RAFT DIBMAs (a) R-D20, (b) R-D32, (c) R-D37, (d) R-D66, (e) R-D88, (f) R-D96 and (g) R-D12. Magnified images show representative single particles of RAFT DIBMA DMPC nanodiscs from the micrograph. DMPC-DIBMALPs were prepared by addition of polymer to DMPC liposomes at a 3:1 polymer to lipid ratio and incubated for 24h to allow for complete solubilization and nanodisc formation. Samples were then negatively stained using uranyl acetate and imaged at 60 kX. (h) Size distribution analysis of DMPC-DIBMALP sizes imaged with TEM plotted as a function of RAFT DIBMA M_n. Points represent the mean frequency of sizes of 250 particles with error bars showing ± 1 standard deviation.

We initially investigated the membrane dissolving properties of RAFT DIBMAs to determine the effect, if any, the chain length or presence of a RAFT group would have on the polymer's ability to solubilize lipids. In order to test this an assay was developed whereby the decrease in turbidity of a solution of liposomes upon addition of a solubilizing copolymer was measured (Figure *4*). The decrease in turbidity is caused by the rapid disruption of the liposomes by the polymer and subsequent formation of smaller nanoscale discs that scatter less light (and hence have a lower turbidity).[19] Alongside comparisons of RAFT DIBMAs, commercial samples of DIBMA and SMA were also analyzed to allow

comparisons between our synthesized polymers and those more readily available commercially. Data in Figure *4* shows the rapid decrease in scattered light of a solution of 1,2-dimyristoyl-sn-glycero-3-phosphocholine (DMPC) liposomes upon addition of copolymers at t = 40 s.

$$\frac{OD_{620}}{OD_{620}^{t=0}} = 1 - C_f e^{-k_f t} - C_s e^{-k_s t} \qquad (1)$$

All RAFT DIBMAs show an initial rapid decrease in the turbidity of the solutions, followed by a longer phase of slower gradual decline; this biphasic behavior was modelled to determine rate constants, with all solubilizations best described by a two-phase decay model in comparison to a one-phase decay model (Figure *4*b). The resultant rate constants for each phase (k_f *and* k_s) were calculated to allow for comparison between polymers. Commercially available SMA (SMA2000P, Cray Valley) and DIBMA (Sokalan-derived) were also analyzed and show the same biphasic decrease in turbidity as the RAFT DIBMAs. k_s values for all RAFT DIBMAs, as well as SMA and Sokalan-derived DIBMA show no significant difference in solubilization rate, whilst k_f values vary more considerably among the different polymers. Figure *4*c shows the k_f values of RAFT DIBMAs plotted as a function of their M_n. It can be seen that the rate is initially high with a k_f of ~7.5 min^{-1} for the shortest chain DIBMA R-D12. This value then appears to drop and stabilize in polymers with M_n 2100 – 7000 g/mol to a k_f of ~ 4 min^{-1}. Long chain RAFT DIBMAs R-D88 and R-D96 show increased k_f values also, similar to the shortest chain DIBMA R-D12. Interestingly, rates for R-D20, R-D32, R-D37 and R-D66 are comparable with that of SMA2000P and Sokalan-derived DIBMA.

The data in Figure *4* highlights the effect of polymer chain length on solubilization. It is clear that all RAFT DIBMAs were capable of solubilizing lipids rapidly in a similar manner to SMA. Previous studies in the literature have revealed that SMA solubilization follows an initial rapid step of polymer adsorption to the lipid membrane, followed by membrane disruption.[20] These two phases of solubilization would perhaps therefore be represented in this system in the biphasic loss of optical

density in vesicles being solubilized by the amphipathic polymers. The initial rapid decrease in turbidity seen in Figure *4*a may be indicative of the process of liposome destabilization, thereby causing an initial large drop in turbidity due to a reduction in the amount of light scattered by the now destabilized membranes.

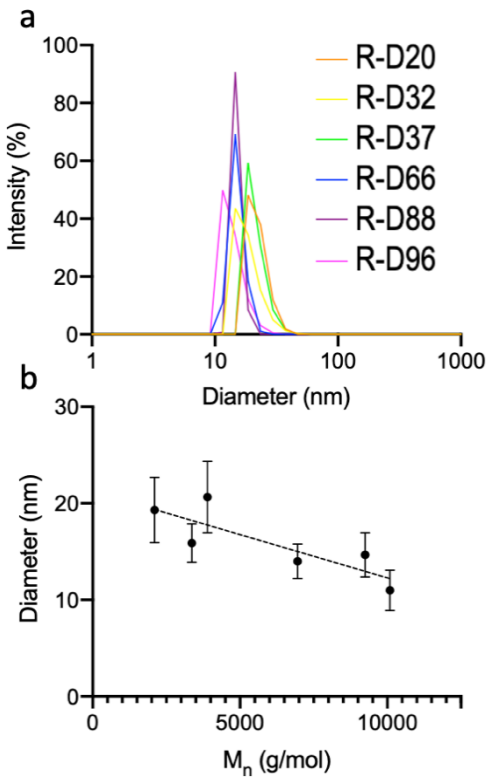

Figure 6 - Structural analysis of DMPC-DIBMALP nanodiscs using dynamic light scattering (DLS). (a) Intensity-based distributions of DMPC liposomes solubilized using RAFT DIBMAs of varying M_n. DMPC-DIBMALPs were prepared by addition of polymer to DMPC liposomes at a 3:1 polymer to lipid ratio and incubated for 24h to allow for complete solubilization and nanodisc formation before DLS measurement. DLS measurements are the result of 10, 1 second accumulations. (b) Hydrodynamic diameter of DMPC-DIBMALPs plotted as a function of the copolymer M_n, points represent the mean of three experiments with error bars representing ± 1 standard deviation.

Following destabilization, SMA nanodiscs are formed and stabilized by the burial of the phenyl groups into the acyl core of the phospholipid bilayer; whilst DIBMA is stabilized in a similar manner using its hydrophobic alkyl chains.[2] The second phase of the model may represent this gradual approach to a homogenous set of discs with a narrow size distribution, driven by lipid exchange among discs. [21] The sharing of the biphasic solubilization profile seen in Figure *4*a by both SMA and DIBMA provides further evidence that the driving forces behind the mechanism of solubilization by these polymers are also shared.

DIBMA nanoparticle characterization

Dynamic light scattering experiments were also performed as an orthogonal technique to TEM for determining the size of nanoparticles. Data in Figure *6*a show the intensity-based distribution of nanoparticles formed using DMPC and RAFT DIBMAs, the data shows a narrow size distribution of particles with Z-averages ranging from 11 – 23 nm, in agreement with TEM-derived particle sizes and with previous reports using DIBMA.[10] DLS measurements of R-D12 revealed a heterogeneous range of particles from 7 – 210 nm. The results here support the idea that the sample consists of a mixture of nanodiscs and disrupted vesicles, as visualized by TEM and seen in Figure *5*g; this corroborates with findings in a similar system using fractionated DIBMA from a commercial source wherein all but the shortest polymer chains were capable of solubilizing and forming nanodiscs.[10]

The presence of pores in vesicles in samples made using R-D12 show that whilst the polymer is capable of entering and solubilizing membranes (Figure *5*), it is incapable of producing a homogenous sample of nanodiscs as seen with other similar polymers (Figure *5*g), the reduction in chain length appears to result in the inability for nanodiscs to separate from the larger pore-containing membrane structures. Therefore, we believe that these pore-containing vesicles represent an intermediary step in liposome solubilization by amphipathic copolymers, with studies in the literature also showing the capability of SMA to form pores in biomembranes[22] as a potential precursor for nanodisc formation. Similar studies have also suggested that the formation of lipid discs can follow an island-formation pathway,[23]

whereby small pores induced by the copolymer eventually merge to leave a lipid disc which is capable of moving out of the bilayer as a lipid-copolymer complex.

One of the primary limitations of SMA is its low tolerance for divalent cations, as well as insolubility at low pH, these limitations can prevent proteins encapsulated in SMALPs from being investigated using various downstream biochemical methods. In order to assess the stability of our RAFT DIBMA nanodiscs an assay was developed wherein solutions of nanodiscs were exposed to varying environmental conditions (pH, $[Ca^{2+}]$ and $[Mg^{2+}]$) and the turbidity of the solution measured. Nanodisc solutions that show an increased turbidimetric signal indicate nanodisc destabilization due to precipitation of the polymer and subsequent precipitation of lipid components from the nanodisc phase. Data in Figure *7*a show that nanodiscs formed using R-D20, the second lowest M_n RAFT DIBMA show stability to pH 5.5, with all other RAFT DIBMAs remaining stable to pH 5. In this experiment SMA acted as a control and precipitated at approximately pH 6, which is consistent with data for SMA-based nanodiscs in the literature.[24] The data from Figure *7*b and c show the sensitivity of RAFT DIBMA nanodiscs to solutions containing the divalent cations magnesium and calcium. All RAFT DIBMA copolymer nanodiscs were resistant to magnesium ions up to a concentration of 8 mM, with SMA based nanodiscs sensitive to low concentrations of magnesium (< 1 mM). In the case of calcium all RAFT DIBMAs however showed increased resistance compared to SMA by remaining stable with up to 4 mM calcium ions in solution.

DIBMA solubilization of membrane proteins from *E. coli*

Both SMA and DIBMA have been shown to be capable of solubilizing membrane proteins directly from biological membranes. We therefore investigated the efficiency of our RAFT DIBMAs to solubilize *E. coli* membranes overexpressed for cell division protein ZipA; having been extensively characterized in SMA previously.[16] The solubilizing ability of RAFT DIBMAs was compared to commercially available SMA2000P and Sokalan, both already commonly utilized in solubilizing functional membrane proteins.

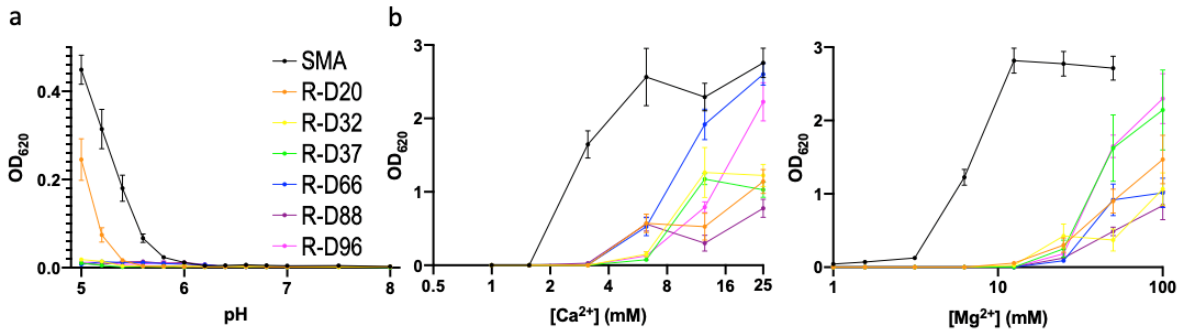

Figure 7. Analysis of RAFT DIBMALP stability. (a) The turbidity of DIBMALP solutions as a function of pH, nanodiscs were prepared by addition of polymer to DMPC liposomes at a 3:1 polymer to lipid ratio in 50 mM Tris, 150 mM NaCl and incubated for 24 h to allow for complete solubilization and nanodisc formation. (b) The turbidity of DIBMALP solutions as a function of calcium and magnesium ion concentration. Points represent the mean value taken from three separate experiments with error bars displaying SEM

After solubilization of the membranes by the various polymers for 24 h, soluble and insoluble fractions were separated by ultracentrifugation and analyzed by SDS-PAGE (Figure *8*a). Samples which successfully solubilized ZipA will produce a band that migrates with an apparent mass of approximately 50 kDa. It should be noted that despite ZipA having a mass of < 40 kDa, ZipA is known to migrate aberrantly through SDS-PAGE gels giving an apparent mass of 40 kDa.[16, 25, 26]

RAFT DIBMA solubilized samples were all shown capable of solubilizing ZipA, with all lanes containing soluble material presenting a band of ~40 kDa. Densitometric analysis of the SDS-PAGE gel (Figure *8*b) reveals a solubilization efficiency for the *E. coli* protein ZipA of ~75% for all RAFT DIBMAs, with no statistically significant difference in solubilization efficiency found among the polymer samples. Solubilization efficiency was also similar amongst RAFT DIBMAs and SMA2000P. The commercially available form of DIBMA, however, is the least efficient at solubilizing ZipA, with an efficiency of ~30%. This lower efficiency for Sokalan-derived DIBMA has previously been reported in studies comparing

SMA and DIBMA and is further corroborated by the data in Figure *8*b showing a reduced rate of solubilization in Sokalan-derived DIBMA compared to SMA. Interestingly, R-D12, R-D20, R-D32 and R-D37 all produce signals from SDS-PAGE free of the smearing characteristic of SDS-PAGE with SMA2000P and Sokalan-derived DIBMA.

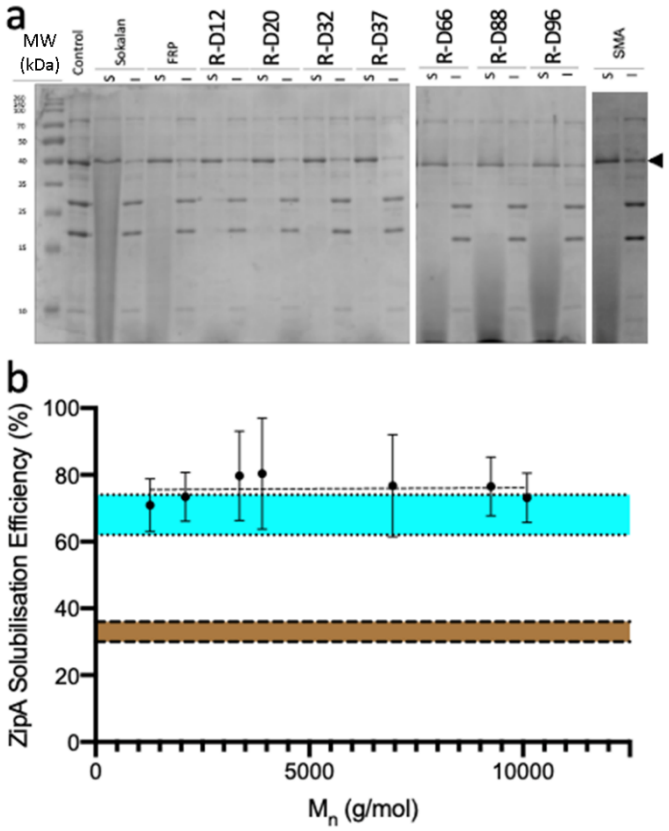

Figure 8. The solubilization of membrane proteins using RAFT DIBMA copolymers. (a) Coomassie stained SDS-PAGE showing proteins both solubilized (S) and remaining insoluble (I) after incubation of E. coli membranes (transformed for overexpression of the transmembrane protein ZipA) with Sokalan-derived DIBMA, conventional radical polymerization (FRP) DIBMA and RAFT DIBMAs of increasing M_n. The black arrow is representative of the ZipA band and a control using total insoluble protein prior to addition of copolymer is also shown. (b) Densitometric analysis of SDS-PAGE showing efficiency of solubilization of the protein ZipA. Solubilization efficiency is expressed as a percentage of total insoluble ZipA, with error bars representing the SEM of three separate experiments.

Smearing can be seen however in the soluble lanes of R-D66, R-D88 and R-D96, with R-D88 also having a *Đ* of 1.7. The smearing therefore is likely caused by incomplete migration of excess polymer present in the sample from the gel. Both commercial SMA and Sokalan-derived DIBMA are copolymers synthesized using conventional radical polymerization, which results in them having a broad molecular weight distribution, therefore SDS-PAGE gels using these copolymers will likely always maintain smearing due to the presence of high molecular weight copolymer chains remaining post-solubilization. The DIBMA copolymers in this study synthesized using RAFT however have comparatively narrower molecular weight distributions, therefore samples R-D12, R-D20, R-D32 and R-D37 represent samples with a low enough M_n and *Đ* that the bulk of excess polymer chains are capable of completely migrating through the gel during the electrophoretic process.

Conclusions

The success of nanoencapsulation systems (like SMALPs or MSPs) for producing membrane proteins in their native environment has been underlined by their use in a steadily increasing number of membrane protein studies. As with any new area that is reliant on a specific reagent, successful application has also led to work on improving the reagent itself. For SMALPs this has led to a rapid introduction of a number of new polymer derivatives.[23] One of the most successful has been the DIBMA polymer which has clear advantages over SMA in terms of divalent cation sensitivity. However, only one preparation of DIBMA is currently available and little is known about whether this form represents the optimal solution.

In this contribution we carried out a systematic analysis of the influence of DIBMA polymer length on nanodisc formation with a view to discovering whether polymer size can influence performance. Our results show that except for the lowest molecular weight the polymers all form recognizable nanodiscs that in general behave in a similar manner to the commercially available material. Kinetically we do observe an influence of polymer size with optimum performance being close to a M_n of 5000.

Our studies of protein solubilization again show very similar protein extraction efficiencies for all polymers tested. However, analysis of PAGE data shows that the lower molecular weight polymers interfere less with the staining of the gels. This is an important observation as visualization of the proteins using PAGE is a fundamental part of any protein purification process.

Finally, our EM studies of the morphology of nanodiscs formed using the polymer highlights a somewhat unexpected result that might provide insights into disc formation. The images for the lowest molecular weight polymer show a state of incomplete membrane protein solubilization. Instead of discs we observe membranes with a "lacey" appearance. Unusually for membranes we observe holes through the bilayer and on the edges of bilayer fragments there is evidence of convex regions. It is possible that what we are observing are the initial stages of disc formation where polymer penetrated the bilayer forming holes.[27] In the case of the edges of bilayer fragments these holes have merged, leading to the production of a fragment. Thus the edges of the fragment appear to be stabilised by the presence of polymer.

Overall, our data shows that there is a "sweet spot" for DIBMA polymers that provide rapid and robust nanodisc formation without perturbing PAGE visualization. We also show initial evidence for the mechanism of DIBMA mediated nanodisc formation.

Conflicts of interest

There are no conflicts to declare.

Acknowledgements

BK, LEB, WH and RP acknowledge support by the South African Research Chairs Initiative of the Department of Science and Technology (DST) and National Research Foundation (NRF) of South Africa (Grant no. 46855).

We acknowledge the Midlands Regional Cryo-EM Facility, hosted at the Warwick Advanced Bioimaging Research Technology Platform, for use of the JEOL 2100Plus, supported by MRC award reference MC_PC_17136

1. Knowles, T. J.; Finka, R.; Smith, C.; Lin, Y. P.; Dafforn, T.; Overduin, M., Membrane proteins solubilized intact in lipid containing nanoparticles bounded by styrene maleic acid copolymer. *J Am Chem Soc* **2009,** *131* (22), 7484-5.
2. Jamshad, M.; Grimard, V.; Idini, I.; Knowles, T. J.; Dowle, M. R.; Schofield, N.; Sridhar, P.; Lin, Y.; Finka, R.; Wheatley, M.; Thomas, O. R. T.; Palmer, R. E.; Overduin, M.; Govaerts, C.; Ruysschaert, J.-M.; Edler, K. J.; Dafforn, T. R., Structural analysis of a nanoparticle containing a lipid bilayer used for detergent-free extraction of membrane proteins. *Nano Research* **2015,** *8* (3), 774-789.
3. Tonge, S. R.; Tighe, B. J., Responsive hydrophobically associating polymers: a review of structure and properties. *Adv Drug Deliv Rev* **2001,** *53* (1), 109-22.
4. Postis, V.; Rawson, S.; Mitchell, J. K.; Lee, S. C.; Parslow, R. A.; Dafforn, T. R.; Baldwin, S. A.; Muench, S. P., The use of SMALPs as a novel membrane protein scaffold for structure study by negative stain electron microscopy. *Biochim Biophys Acta* **2015,** *1848* (2), 496-501.
5. Parmar, M.; Rawson, S.; Scarff, C. A.; Goldman, A.; Dafforn, T. R.; Muench, S. P.; Postis, V. L. G., Using a SMALP platform to determine a sub-nm single particle cryo-EM membrane protein structure. *Biochim Biophys Acta* **2018,** *1860* (2), 378-383.
6. Dörr, J. M.; Koorengevel, M. C.; Schäfer, M.; Prokofyev, A. V.; Scheidelaar, S.; van der Cruijsen, E. A. W.; Dafforn, T. R.; Baldus, M.; Killian, J. A., Detergent-free isolation, characterization, and functional reconstitution of a tetrameric K⁺ channel: The power of native nanodiscs. *Proceedings of the National Academy of Sciences* **2014,** *111* (52), 18607.
7. Broecker, J.; Eger, B. T.; Ernst, O. P., Crystallogenesis of Membrane Proteins Mediated by Polymer-Bounded Lipid Nanodiscs. *Structure* **2017,** *25* (2), 384-392.
8. Cunningham, B. C.; Wells, J. A., Comparison of a structural and a functional epitope. *J Mol Biol* **1993,** *234* (3), 554-63.
9. Grethen, A.; Oluwole, A. O.; Danielczak, B.; Vargas, C.; Keller, S., Thermodynamics of nanodisc formation mediated by styrene/maleic acid (2:1) copolymer. *Sci Rep* **2017,** *7* (1), 11517.
10. Oluwole, A. O.; Klingler, J.; Danielczak, B.; Babalola, J. O.; Vargas, C.; Pabst, G.; Keller, S., Formation of Lipid-Bilayer Nanodiscs by Diisobutylene/Maleic Acid (DIBMA) Copolymer. *Langmuir* **2017,** *33* (50), 14378-14388.
11. Oluwole, A. O.; Danielczak, B.; Meister, A.; Babalola, J. O.; Vargas, C.; Keller, S., Solubilization of Membrane Proteins into Functional Lipid-Bilayer Nanodiscs Using a Diisobutylene/Maleic Acid Copolymer. *Angew Chem Int Ed Engl* **2017,** *56* (7), 1919-1924.
12. Moad, G.; Rizzardo, E.; Thang, S. H., Toward living radical polymerization. *Acc. Chem. Res.* **2008,** *41* (9), 1133-1142.
13. Perrier, S., 50th Anniversary Perspective: RAFT Polymerization—A User Guide. *Macromolecules* **2017,** *50* (19), 7433-7447.
14. Ma, J.; Cheng, C.; Sun, G.; Wooley, K. L., A polarity-activation strategy for the high incorporation of 1-alkenes into functional copolymers via RAFT copolymerization. *J. Polym. Sci., Part A: Polym. Chem.* **2008,** *46* (11), 3488-3498.
15. Postma, A.; Davis, T. P.; Evans, R. A.; Li, G.; Moad, G.; O'Shea, M. S., Synthesis of well-defined polystyrene with primary amine end groups through the use of phthalimido-functional RAFT agents. *Macromolecules* **2006,** *39* (16), 5293-5306.
16. Lee, S. C.; Collins, R.; Lin, Y.-p.; Jamshad, M.; Broughton, C.; Harris, S. A.; Hanson, B. S.; Tognoloni, C.; Parslow, R. A.; Terry, A. E.; Rodger, A.; Smith, C. J.; Edler, K. J.; Ford,

R.; Roper, D. I.; Dafforn, T. R., Nano-encapsulated Escherichia coli Divisome Anchor ZipA, and in Complex with FtsZ. *Scientific Reports* **2019,** *9* (1), 18712.
17. Baussard, J. F.; Habib-Jiwan, J. L.; Laschewsky, A.; Mertoglu, M.; Storsberg, J., New chain transfer agents for reversible addition-fragmentation chain transfer (RAFT) polymerisation in aqueous solution. *Polymer* **2004,** *45* (11), 3615-3626.
18. Skrabania, K.; Miasnikova, A.; Bivigou-Koumba, A. M.; Zehm, D.; Laschewsky, A., Examining the UV-vis absorption of RAFT chain transfer agents and their use for polymer analysis. *Polymer Chemistry* **2011,** *2* (9), 2074-2083.
19. Dörr, J. M.; Scheidelaar, S.; Koorengevel, M. C.; Dominguez, J. J.; Schäfer, M.; van Walree, C. A.; Killian, J. A., The styrene-maleic acid copolymer: a versatile tool in membrane research. *Eur Biophys J* **2016,** *45* (1), 3-21.
20. Scheidelaar, S.; Koorengevel, M. C.; Pardo, J. D.; Meeldijk, J. D.; Breukink, E.; Killian, J. A., Molecular model for the solubilization of membranes into nanodisks by styrene maleic Acid copolymers. *Biophys J* **2015,** *108* (2), 279-90.
21. Cuevas Arenas, R.; Danielczak, B.; Martel, A.; Porcar, L.; Breyton, C.; Ebel, C.; Keller, S., Fast Collisional Lipid Transfer Among Polymer-Bounded Nanodiscs. *Sci Rep* **2017,** *7*, 45875.
22. Orwick Rydmark, M.; Christensen, M. K.; Köksal, E. S.; Kantarci, I.; Kustanovich, K.; Yantchev, V.; Jesorka, A.; Gözen, I., Styrene maleic acid copolymer induces pores in biomembranes. *Soft Matter* **2019,** *15* (39), 7934-7944.
23. Stroud, Z.; Hall, S. C. L.; Dafforn, T. R., Purification of membrane proteins free from conventional detergents: SMA, new polymers, new opportunities and new insights. *Methods* **2018**.
24. Hall, S. C. L.; Tognoloni, C.; Price, G. J.; Klumperman, B.; Edler, K. J.; Dafforn, T. R.; Arnold, T., Influence of Poly(styrene- co-maleic acid) Copolymer Structure on the Properties and Self-Assembly of SMALP Nanodiscs. *Biomacromolecules* **2018,** *19* (3), 761-772.
25. Mosyak, L.; Zhang, Y.; Glasfeld, E.; Haney, S.; Stahl, M.; Seehra, J.; Somers, W. S., The bacterial cell-division protein ZipA and its interaction with an FtsZ fragment revealed by X-ray crystallography. *EMBO J* **2000,** *19* (13), 3179-91.
26. Kuchibhatla, A.; Bhattacharya, A.; Panda, D., ZipA binds to FtsZ with high affinity and enhances the stability of FtsZ protofilaments. *PLoS One* **2011,** *6* (12), e28262.
27. Xue, M.; Cheng, L.; Faustino, I.; Guo, W.; Marrink, S. J., Molecular Mechanism of Lipid Nanodisk Formation by Styrene-Maleic Acid Copolymers. *Biophys. J.* **2018,** *115* (3), 494-502.

Supporting Information for:

Influence of DIBMA polymer length on lipid nanodisc formation and membrane protein extraction

Lauren E. Ball, Liam J. Riley, Waled Hadasha, Rueben Pfukwa, Corinne J. I. Smith, Tim R. Dafforn* and Bert Klumperman*

Calculation of monomer conversion from ^{1}H NMR spectra is conducted according to Equation S1.

$$Conversion = 1 - \frac{\left(\frac{I_{1Hmonomer}}{I_{1Htriox}}\right)_t}{\left(\frac{I_{1Hmonomer}}{I_{1Htriox}}\right)_0} \quad \text{(S1)}$$

Theoretical number average molar mass of RAFT made polymer is approximated according to Equation S2.

$$M_{n,target} = \frac{[M_{MAnh}]_0 . p}{[RAFT]_0} . MW_{MAnh} + \frac{[M_{DIB}]_0 . p}{[RAFT]_0} . MW_{DIB} + MW_{RAFT} \quad \text{(S2)}$$

Exponential decay equation used to model for SMA and DIBMA-induced solubilisation (Equation 3).

$$Y = Y_{t=\infty} + s_f e^{(-k_f X)} + s_s e^{(-k_s X)}$$

k_s and k_f are the two rate constants, expressed in reciprocal of the X axis time units

Table S1. Conversion and molecular weight data for RAFT copolymerisations performed using varying monomer ratios.

Sample	Monomer ratio (DIB: MAnh)	[a] DIB conversion (%)	[a] MAnh conversion (%)	[b] M_n^{theo} (kDa)	[c] DIB units	[c] MAnh units	M_n^{NMR} (kDa)	[d] M_n^{SEC} (kDa)	*Đ*
R-D20	50:50	71	55	1.6	12	10	2.1	3.2	1.24
R-D37A	75:25	22	42	3.2	19	18	3.9	4.9	1.31
R-D54A	25:75	84	33	5.1	28	26	5.7	7.4	1.32

a-Conversion determined using ^{1}H NMR spectroscopy and an internal reference (1,3,5-trioxane)
b-Theoretical M_n calculated using individual DIB and MAnh conversions

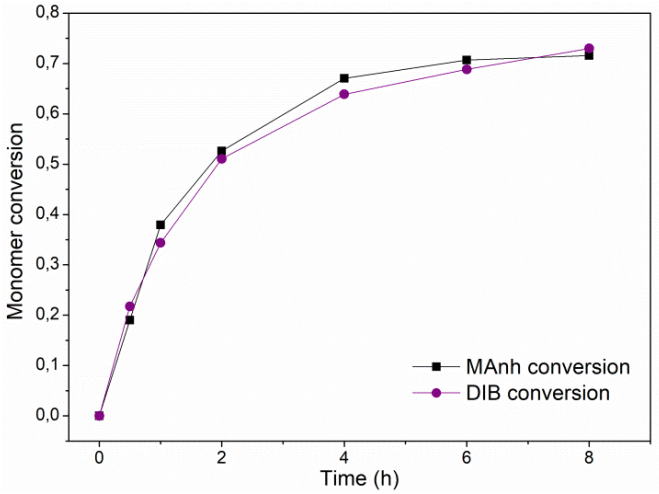

Figure S1. Monomer conversion vs time for the RAFT mediated polymerisation of DIB and MAnh (sample R-D22).

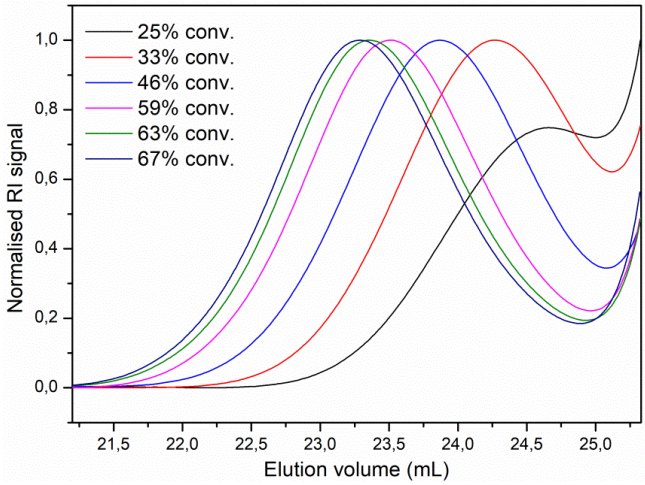

Figure S2. SEC curves for R-D41 kinetic samples. Kinetic samples were taken at specified time intervals and analysed using SEC with DMF as mobile phase and PMMA calibration standards.

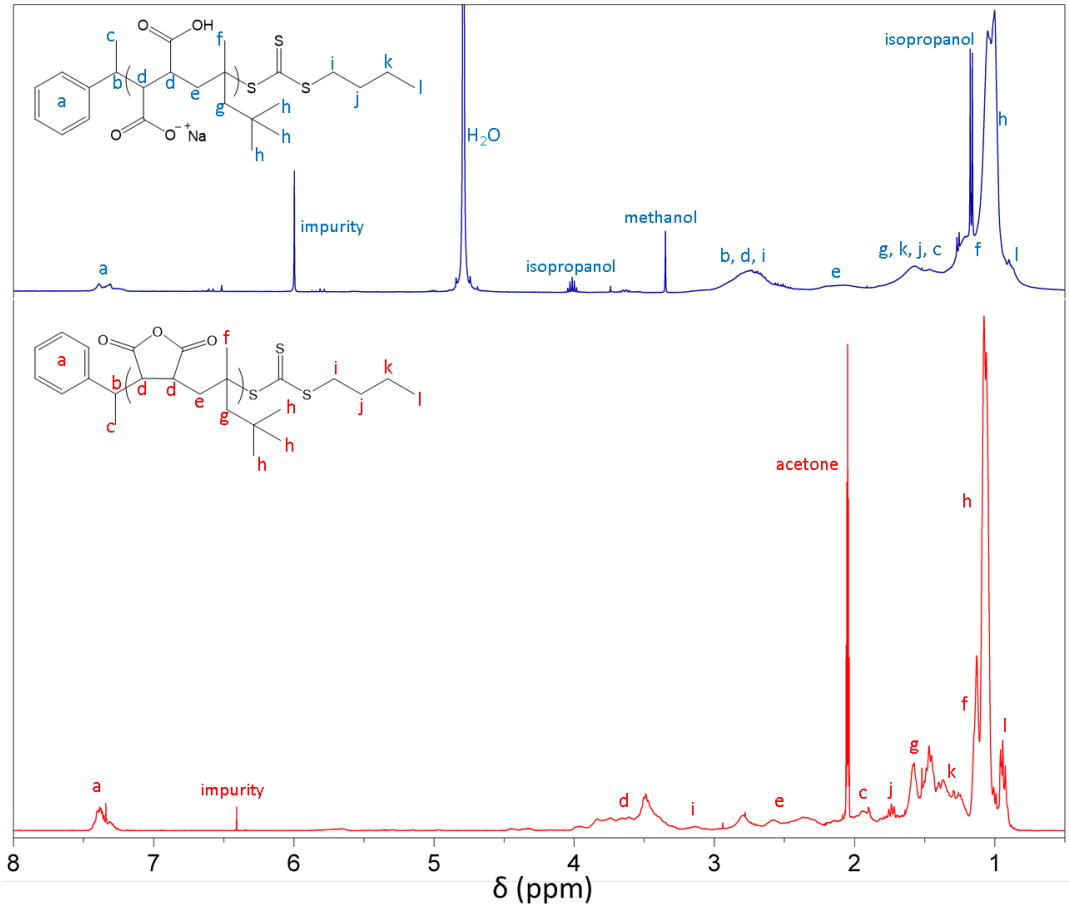

Figure S3. ^{1}H NMR Spectra of DIBMA sample R-D20 before (red) and after (blue) hydrolysis of the MAnh residues.